

Downsizing of In-vehicle DC/DC Converters with GaN Devices

Keiji TASHIRO*, Yusuke OKAGAWA, Kuiyuan ZHANG, Yukinori YAMADA, Shinsuke TACHIZAKI, and Seiji TAKAHASHI

Electric vehicles and hybrid electric vehicles are in widespread use and these vehicles are all equipped with DC/DC converters for charging lead-acid batteries from high-voltage storage batteries. To simplify the installation, DC/DC converters are required to be small. This paper describes a DC/DC converter that has been downsized by 50% compared with conventional ones by increasing the switching frequency from 100 kHz to 500 kHz using GaN devices.

Keywords: GaN, high frequency, electric vehicle, DC/DC converter

1. Introduction

In recent years, the rise in environmental awareness in society has accelerated the widespread use of electric vehicles, including hybrid electric vehicles. Each of these electric vehicles is equipped with a DC/DC converter (hereinafter referred to as the “converter”) for charging a 12-V lead-acid battery from a high-voltage storage battery (Fig. 1) that powers a traction motor. For easier installation into vehicles, the converters are strongly required to be downsized. In this paper, development for the downsizing of a converter is discussed.

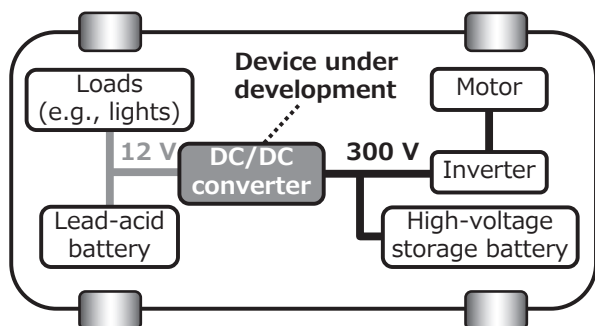


Fig. 1. Electric vehicle power system diagram

2. Development Goal

2-1 Development specifications

Table 1 presents the specification values of the new converter we developed. Currently, converters available on the market are rated mostly at a maximum output current of 100 to 150 A. In the future, as driver-assistance systems and on-board entertainment devices will be increasingly introduced, current consumption demand of the 12-V power system will increase. To respond to this need, we set the maximum output current of the newly developed converter to 200 A. Moreover, to support power supply redundancy and additional increases in current consump-

Table 1. Specifications of newly developed converter

Items	Value
Input Voltage	240 ~ 400 Vdc
Output voltage	10 ~ 15 Vdc
Output Current	~ 200 A
Cooling condition	Forced air cooling (40°C, 1 m ³ /min)

tion, we designed the converter to allow for the connection of multiple converter units for parallel operation. For cooling system, we invented a structure compatible with both water and air cooling systems, ensuring interchangeability between a water jacket and cooling fins. We designed the converter ensuring thermal feasibility, even with forced air cooling with relatively low cooling capacity.

Figure 2 shows the market trends regarding converter output power density, as investigated by Sumitomo Electric Industries, Ltd. From the perspective of ensuring easier installation into vehicles, the trend in converters is towards high output power density, i.e., the downsizing of the unit size per unit output. With this in mind, we set the development target to 6 W/cc, which substantially exceeds the output power density of the existing products. This is a challenging goal relative to the levels of mass-production converters launched by competitors, being equivalent to downsizing the unit to a half or smaller.

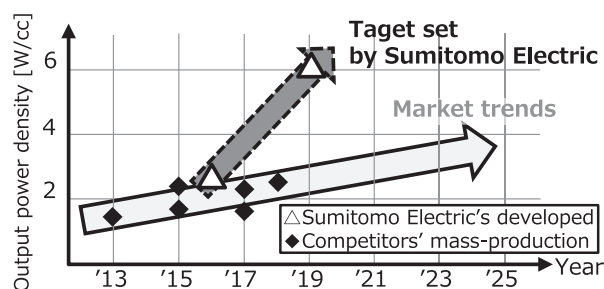


Fig. 2. Trends in converter output power density

2-2 Development concept

The block diagram of the converter is illustrated in Fig. 3. In a converter, magnetic parts, such as a transformer and filter coil, occupy a large space. While existing converters generally have a switching frequency of 100 kHz, Sumitomo Electric has set a direction to downsize the coil components to achieve the target unit size by substantially raising the switching frequency.

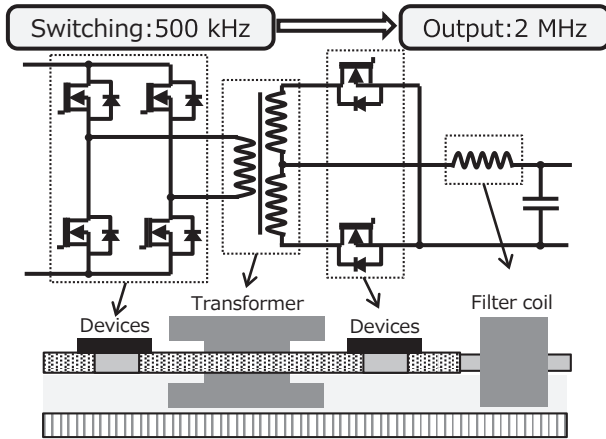


Fig. 3. Block diagram of converter

Meanwhile, high switching frequency causes following problems: (I) an increase in loss attributable to semiconductor devices and (II) an increase in electromagnetic noise. To tackle (I), we adopted gallium nitride (GaN) devices, which are better in high-frequency characteristics than conventional silicon (Si) devices, to reduce loss, downsize the unit, and achieve power conversion efficiency comparable to or better than that of the existing products. Regarding (II), the International Special Committee on Radio Interference (CISPR) 25⁽¹⁾ standards serve as noise design guidelines for in-vehicle products. For converters in particular, the major challenge involved in the use of higher frequencies is compliance with the standards applicable to the medium wave (MW) band (530–1,800 kHz) used for amplitude modulation (AM) radio. With this in mind, we set the switching frequency to 500 kHz, and the ripple*¹ frequency superimposed on the output cable to 2 MHz. By setting these frequencies, which are major noise sources, and avoiding the MW frequency band, the developed converter can meet the noise standards with the minimum required filter parts.

In general, downsizing a unit results in a close-packed heat-generating components, which make it difficult to reduce component temperatures below the permissible limits (i.e. achieving thermal feasibility). Consequently, for this developed converter, we selected low-profile components to downsize the unit in height and provide an adequate heat sink area for radiation. These enabled the heat-generating components to be placed in a dispersed manner, achieving both the downsizing of the unit and thermal feasibility.

3. Detailed Design

3-1 Circuit design

Table 2 lists the characteristics of Si devices that are widely used in existing converters and those of GaN devices. Compared with Si devices, GaN devices exhibit a fast switching rate, thus enabling reduced switching loss*². However, the high-speed operation results in high noise levels. In addition, a low gate threshold voltage for on/off switching operation tends to cause unintended device on/off operation (false operation) (Fig. 4). Accordingly, GaN devices may make false operation, even with slight noise arising from the coupling between copper traces, which would not be possible to occur with the use of Si devices. Sumitomo Electric conducted simulations, taking into account even the effects of wiring patterns to optimize circuit constants and copper patterns. This optimization enabled the GaN device to exhibit high-speed operation characteristics at a maximum level while avoiding false operations.

Table 2. Semiconductor device characteristics

	Si	GaN
Switching rate*	1.0	3.5
Gate threshold	3.0 V	1.3 V

*Normalized by Si device value as 1.0

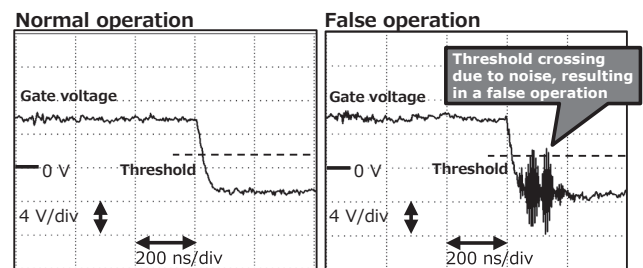


Fig. 4. False operation waveforms of GaN device

3-2 Transformer design

Figure 5 presents transformer coil structures. Many conventional converters have a structure that uses round wires as their transformer coils. However, at high frequen-

Coil structure	Round wire	Litz wire	Board
Schematic diagram	 Core Coil $\Phi 1 \sim 2$ mm	 Enlarged view Approx. $\Phi 0.1$ mm	 Printed circuit board Approx. 0.1-mm thick
Loss	Large (poor)	Small (good)	Small (good)
Cost	Low (good)	High (poor)	Low (good)

Adopted structure

Fig. 5. Transformer coil structure

cies, this structure reduces the effective cross-sectional area of copper due to the skin effect^{*3}, resulting in greater loss. There is the litz wire structure, which utilizes thin stranded wires with approximately 0.1 mm in diameter, to reduce the skin effect. However, this is more costly than the round wire structure. As a solution, Sumitomo Electric adopted a board transformer structure that is assembled with a coil using a copper foil pattern on a printed circuit board, instead of litz wires. This structure enables transformer coils and the mounting board of electronic components to be integrally molded, thus reducing the costs. Moreover, it forms coils by laminating thin conductors with approximately 0.1-mm thick. Therefore, as with litz wires, it is less susceptible to the skin effect, thereby reducing loss.

Meanwhile, losses in high-frequency transformers vary substantially, depending on the shapes of the core and relative positions between the core and the coils. Using the electromagnetic analysis techniques fostered through Sumitomo Electric's in-house reactor development,^{(2),(3)} we analyzed the magnetic flux flows (Fig. 6). Through an optimal design, such as controlling magnetic flux leakage from the core, we reduced loss in the transformer.

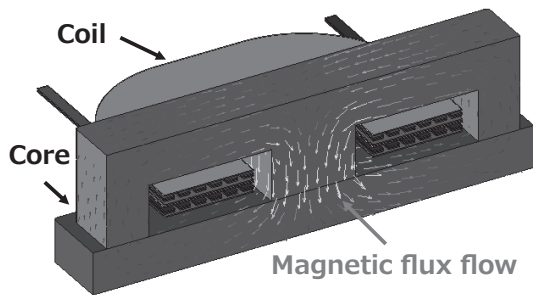


Fig. 6. Analyzed magnetic flux flow of transformer

3-3 Filter coil design

Figure 7 shows the filter coil structures. By raising the switching frequency, the necessary inductance^{*4} of the filter coil can be reduced. Therefore, while a conventional converter has a structure that a purpose-designed copper material is wound several turns around a core to obtain required inductance, the developed converter adopts a structure that a straight copper wiring material is covered with a core. This design allows shared use of wiring parts and filter components so that the space inside the unit can be used efficiently, thereby contributing to downsizing.

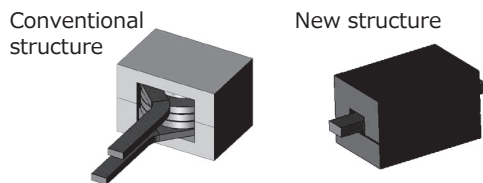


Fig. 7. Filter coil structure

Moreover, since it eliminates a process of winding the copper material, we can reduce manufacturing cost.

3-4 Thermal design

As heat dissipation structures for semiconductor devices, there are the lead mounting structure (Fig. 8 (a)), in which the component has metal pieces for heat dissipation, and the module structure (Fig. 8 (b)), in which the semiconductor chip is mounted on an insulation layer with high thermal conductivity. However, the problem associated with these structures is that leads and wire bonding cause large trace inductance^{*5}, interfering the high-frequency operation of GaN. Meanwhile, as a structure with minimum trace inductance, there is the surface mount structure (Fig. 8 (c)) that eliminates component lead portions, to directly mount the component on a printed circuit board. This structure, however, provides poor heat dissipation performance due to the presence of a plastic printed circuit board material with low-thermal conductivity, intervening on the heat dissipation path. As a solution to these problems, we adopted a structure (Fig. 8 (d)) that a metal piece is placed directly under the surface-mounted device. This design ensured high heat dissipation performance and low trace inductance.

Structure	(a) Lead mounted	(b) Module
Schematic diagram		
Heat dissipation	High (good)	Very high (excellent)
Trace inductance	Large (poor)	A little large (fair)
Cost	Low (good)	High (poor)
Structure	(c) Surface mounted	(d) Surface mounted + Metal piece
Schematic diagram		
Heat dissipation	Low (poor)	High (good)
Trace inductance	Low (good)	Low (good)
Cost	Low (good)	Low (good)

Adopted structure

Fig. 8. Semiconductor device heat dissipation structure

4. Prototype Development and Evaluation Results

4-1 Unit structure and thermal characteristics

Photo 1 shows the appearance of the newly developed converter. By using GaN devices and raising the switching frequency, we downsized the transformer and the filter coil, and lowered the unit height. We realized a 3-kW output converter with a size of $229 \times 116 \times 18.5 \text{ mm} = 491 \text{ cc}$ (excluding the air cooling fins and projections), achieving

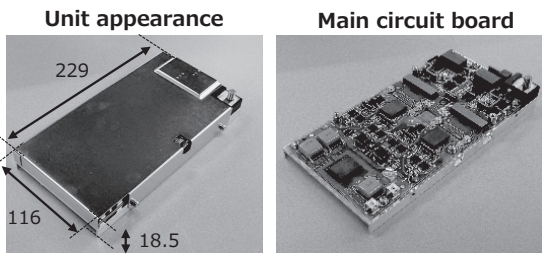


Photo 1. Newly developed DC/DC converter

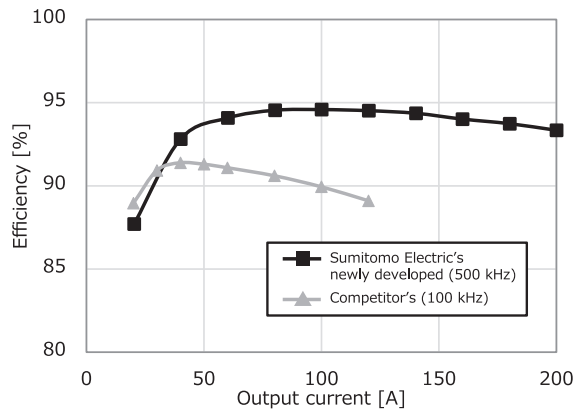


Fig. 10. Efficiency data

the output density target of 6 W/cc.

Figure 9 presents the temperature increase test results obtained at room temperature. Differences between the cooling air temperature and components temperatures, ΔT , are also presented in the figure, noting only the principal heat-generating components: the device and the coil parts. The acceptance/rejection criterion was set to $\Delta T \leq 95^\circ\text{C}$ so that thermal feasibility will hold under the forced air cooling condition of 40°C , while tentatively setting an upper limit of 135°C to provide a margin with respect to the components' temperature rating of 150°C . Temperature increases saturated at an output of 175 A suggests expected thermal feasibility even under continuous operating conditions. At an output of 200 A, the device temperature continued to increase, but there was a good possibility of providing thermal feasibility with operation for about 10 min. The device will be protected if long-term operation is required. This will be done by detecting exceeding temperature increases and controlling the output power.

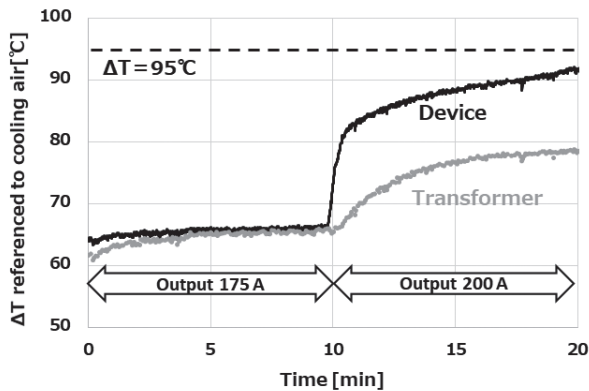


Fig. 9. Temperature increases in principal heat-generating components

competitor's 100-kHz converter, even with the switching frequency raised to 500 kHz.

Next, Fig. 11 gives conducted emission data as noise characteristics. Sumitomo Electric's newly developed converter exhibited wider peaks separation than those of the competitor's converter due to higher switching frequency of 500 kHz. We achieved the noise levels comparable to CISPR 25 Class 3 at both high-voltage input and low-voltage output sides.

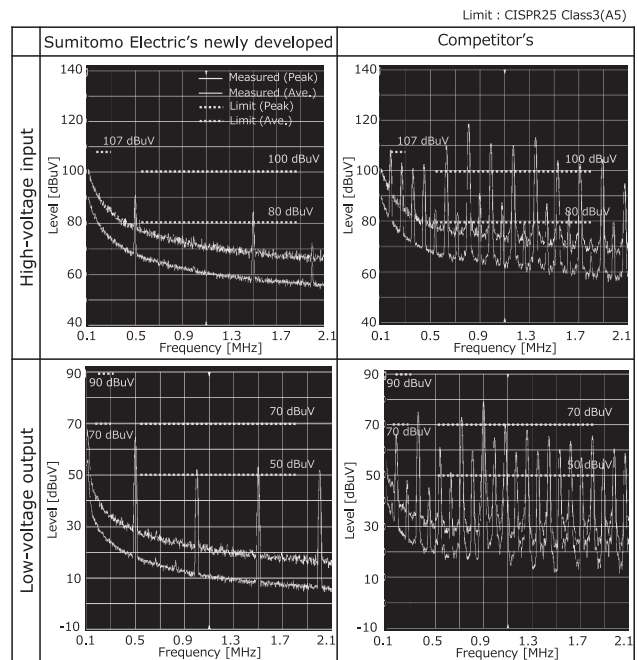


Fig. 11. Conducted emission data

4-2 Electrical characteristics

Electrical characteristics used to determine converter performance generally include power conversion efficiency, noise, and load transient response. First, Fig. 10 provides efficiency data observed when operating converters at an input voltage of 300 V and output voltage of 14 V. With the GaN devices and optimal design of a high-frequency transformer, our newly developed converter was able to achieve an efficiency level higher than that of a

Figure 12 shows the output voltage response, observed as a load transient response when the load current rapidly changed from 5 to 100 A. The slew rate of load current change was set to 800 A/ms, which was sufficiently above the maximum rate of change expected in the actual

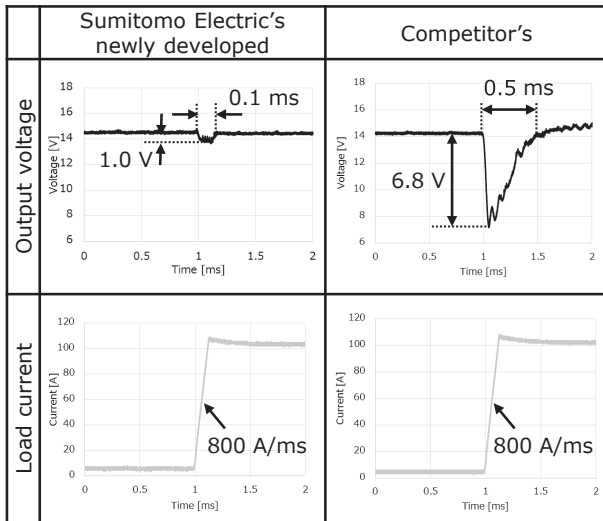


Fig. 12. Load transient response

operation. Our newly developed converter was able to improve voltage control response by raising the switching frequency, allowing to suppress both the output voltage fluctuation range and fluctuation duration in comparison with the competitor's converter. This capability can reduce the risks of load equipment undergoing an abnormal shut-down due to voltage drops.

5. Parallel Operation

While parallel operation of converters can handle load current larger than the maximum output current per unit, existing in-vehicle converters are adapted to constant-voltage (CV) control and have difficulty in parallel operation. In CV control, current flows intensively from the higher-voltage unit when a variation in output voltage occurs due to a sensor error (Fig. 13). This results in an

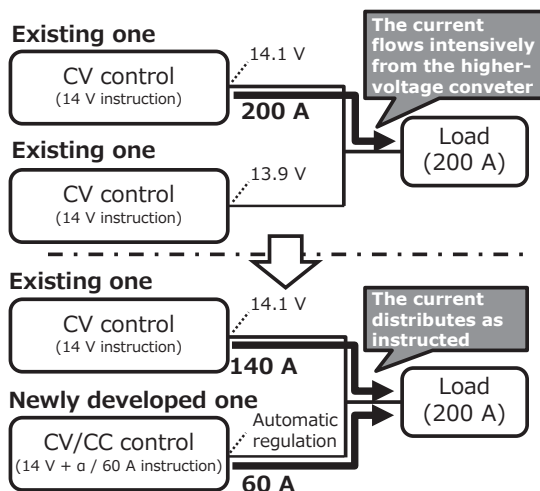


Fig. 13. Parallel converter operations

excessive temperature increase or accelerated degradation.

As a solution to this issue, the newly developed converter incorporated constant-voltage/constant-current (CV/CC) control. By instructing the output voltage higher than that of existing CV unit, CV/CC control unit can automatically regulate the output voltage to ensure an output current as instructed. Thus, load current of two units can be distributed at an appropriate ratio. This CV/CC control can be incorporated into Si device-based converters, as well as GaN device-based converters.

Figure 14 shows the current waveforms in parallel operation of an existing converter available on the market and of Sumitomo Electric's newly developed converter, observed in a verification test of parallel operation. As an example of load current distribution, a current instruction was given so that the current ratio of the existing converter to the newly developed one became 5 : 2 (71% : 29%). In three different load current patterns, the load distribution was within an error range of 1% to 2%, demonstrating operation as envisioned.

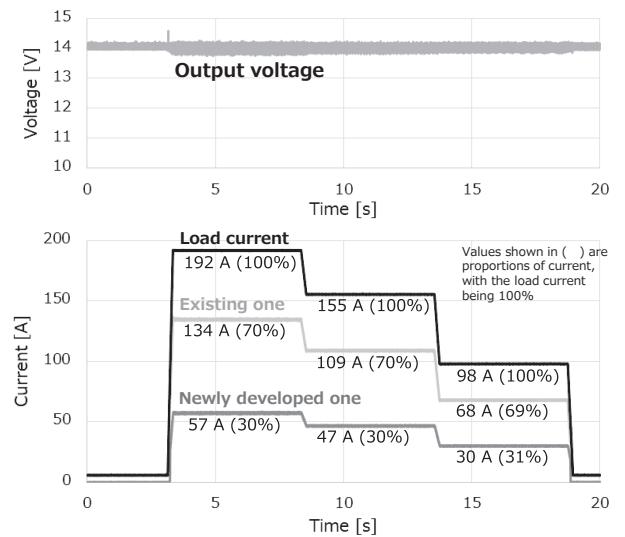


Fig. 14. Verification of actual converters in parallel operation

6. Conclusion

By increasing the switching frequency with GaN devices, our newly developed converter achieved an output density of 6 W/cc, which outperforms the market trends. The newly developed converter has a low-profile structure, 18.5 mm in height, so that it can be installed in a space underneath a vehicle floor. This allows a higher flexibility of installation, as compared with the existing products. Regarding power conversion efficiency and noise, being issues in a higher switching frequency converter, the newly developed converter achieved comparable or better performance than the competitor's. For future development, we intend to work on system designs tailored to in-vehicle installations.

Technical Terms

- *1 Ripple: Pulsating current or voltage produced by converter operation
- *2 Switching loss: A power loss occurring when switching a semiconductor device on/off in a converter. Switching loss increases in proportion to the number of on/off switching cycles per second (switching frequency).
- *3 Skin effect: A phenomenon of an electric current concentrating close to the conductor surface due to a generated magnetic flux. It is observed when passing a high-frequency current through a conductor. This phenomenon results in a reduced effective cross-sectional area for current passage, augmenting losses.
- *4 Inductance: A circuit component property to impede the flow of a high-frequency current. The use of a filter part with high inductance is effective for reducing the emission of high-frequency noise.
- *5 Trace inductance: An inductance component exhibited by part leads and wiring connections. Trace inductance values increase generally with each smaller cross-sectional area and longer wire lengths.

References

- (1) CISPR25:2016, Vehicles, boats and internal combustion engines - Radio disturbance characteristics - Limits and methods of measurement for the protection of on-board receivers
- (2) T. Kanto, et al., "Electromagnetic and Thermal Design Technology for Reactor Development," SEI TECHNICAL REVIEW, No. 70 (April 2010)
- (3) S. Yamamoto, et al., "Small and Lightweight Reactor for Boost Converter," SEI TECHNICAL REVIEW, No. 79 (October 2014)

Contributors The lead author is indicated by an asterisk (*).

K. TASHIRO*

• CAS-EV Development Promotion Division



Y. OKAGAWA

• CAS-EV Development Promotion Division



K. ZHANG

• Ph.D.
CAS-EV Development Promotion Division



Y. YAMADA

• Assistant Manager, CAS-EV Development Promotion Division



S. TACHIZAKI

• Assistant General Manager, CAS-EV Development Promotion Division



S. TAKAHASHI

• Group Manager, CAS-EV Development Promotion Division

